Available online at www.sciencedirect.com
SCIENCE DIRECT®
Journal of Power Sources 133 (2004) 223–228
JOURNAL OF POWER SOURCES
www.elsevier.com/locate/jpowsour

Development of fuel-cell-powered electric bicycle

J.J. Hwang [a,*], D.Y. Wang [a], N.C. Shih [a], D.Y. Lai [b], C.K. Chen [b]

[a] *Research Center for Advanced Science and Technology, Mingdao University, Peetou, Changhua 523, Taiwan*
[b] *Department of Mechanical Engineering, National Cheng Kung University, Tainan 701, Taiwan*

Received 20 November 2003; accepted 6 February 2004

Available online 17 April 2004

Abstract

The design, fabrication, and testing of a prototype of electric bicycle powered by a proton exchange membrane fuel cell (PEMFC) is reported. The fuel-cell system is composed of a 300-W fuel-cell stack, metal hydride canisters, air pumps, solenoid valves, cooling fans, pressure and temperature sensors, and a microcontroller. To reduce cost, all components are commercially available except for the microcontroller, which has been developed to operate the system effectively. The fuel-cell system is installed on a commercial electric bicycle. Results show that the efficiency of the fuel-cell system can reach up to 35%, and the ratio of travel distance to fuel consumption of the prototype electric bicycle is about 1.35 km g^{-1} H_2.

Keywords: Proton exchange membrane fuel cell; Electric bicycle; Microcontroller; Metal hydride; Efficiency; Fuel consumption

1. Introduction

Power-assisted bicycles (PABs) offer a cheap and efficient mode of transportation. They are becoming increasingly popular in many countries. In Asia (e.g., Taiwan), PABs are commonly used on a daily basis for commuting, while people in North America and Europe use them mainly for recreation purposes. Typically, a PAB uses a low-power source to turn a small motor attached to the wheel at the hub or at the tire. In most PABs, the rider can pedal in combination with the power source to magnify power to the wheel. Usually, electric PABs are powered by either lead–acid or nickel–cadmium batteries, with motor power ratings between 200 and 400 W, depending on the make and type. Recently, the fuel cell has been considered as a means to provide direct power to PABs, or more likely to charge the battery which, in turn, drives the motor.

Mingdao University commenced the research and development of a fuel-cell, lightweight vehicle in 2000. In the first phase, as presented in this paper, a 300-W fuel-cell stack has been used for the construction of an easy-to-use, robust, safe power generator installed on a commercial electric bicycle. Wherever possible, the components chosen for the fuel-cell system are commercially available. Only the single-chip microcontroller has been developed, which starts, monitors, and shuts down the fuel-cell system. The bicycle is a low-cost prototype without optimization of weight, dimension, and configuration. It is hoped that this prototype will encourage public acceptance of the technology and will accelerate national licensing processes. The ultimate goal is to bring the fuel-cell technology out of the laboratory and into the marketplace for use in transportation as well as power generation.

2. System design

The conceptual process and instrument design of the fuel-cell system is shown in Fig. 1.

2.1. Fuel-cell stack and power management

The specifications of the fuel-cell stack (made by H-power) utilized in the electric bicycle are listed in Table 1. The stack consists of 40 cells with nominal and peak power of 303 W (0.7 V) and 378 W (0.66 V), respectively. The performance curve of this stack, is shown in Fig. 2 [1]. The stack not only drives the electric motor of the bicycle but also powers other sub-systems. As listed in Table 2, the components in the present system include an electric motor, two air pumps, two solenoid valves, four cooling fans, and a microcontroller. The electric motor can operate under a wide range of voltage, and thus it is directly powered

* Corresponding author. Tel.: +886-488-76660; fax: +886-488-79050.
E-mail address: azaijj@mdu.edu.tw (J.J. Hwang).

0378-7753/$ – see front matter © 2004 Elsevier B.V. All rights reserved.
doi:10.1016/j.jpowsour.2004.02.004

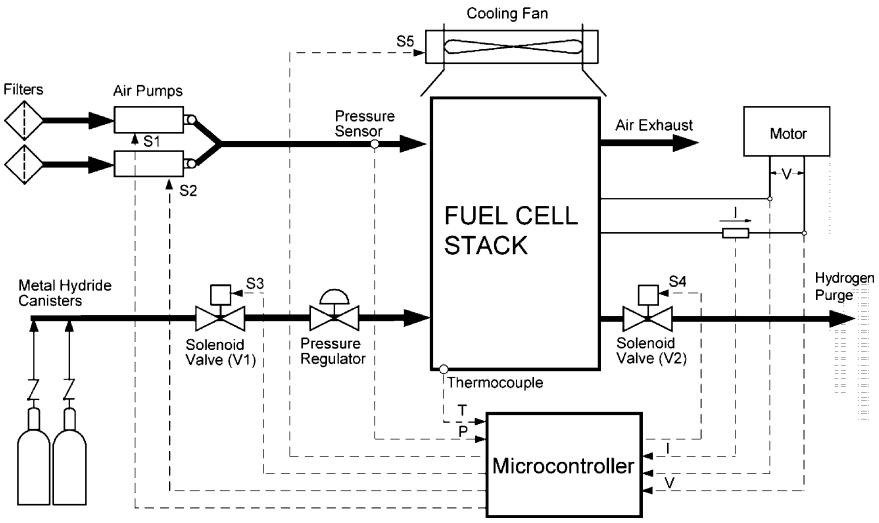

Fig. 1. Fuel cell system.

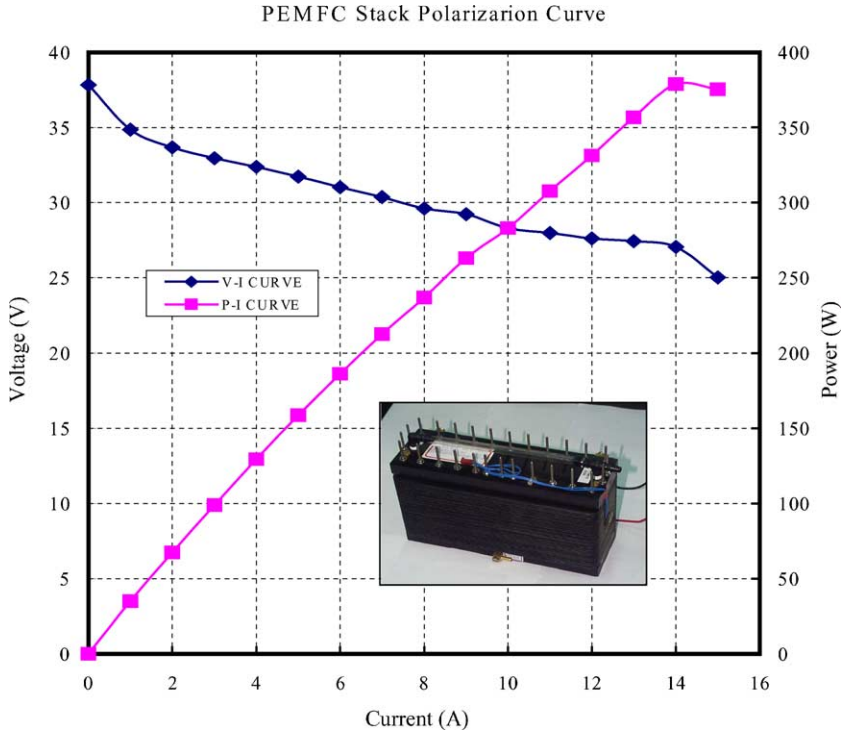

Fig. 2. Voltage–current curve of PEMFC stack.

Table 1
Characteristic data of fuel-cell stack

Specification	
Number of cells	40
Nominal power (W) (at 0.7 V)	303
Nominal voltage (V)	28
Nominal current (A)	11
Peak power (W)	378
Operation conditions	
Stoichiometric ratio of oxidant	2.5
Anodic inlet pressure (psig)	7
Cathodic inlet pressure (psig)	3
Temperature (stack surface) (°C)	40

Table 2
Electric specification of the power-consumed components of fuel-cell system

Component	Number	Specification (V/A)	Power consumption (W)
Motor	1	24/9.5	230
Air pumps	2	12/1.1	26.4
Solenoid valves	2	12/0.12	2.8
Cooling fans	4	12/0.15	7.2
Microcontroller	1	12/2	24

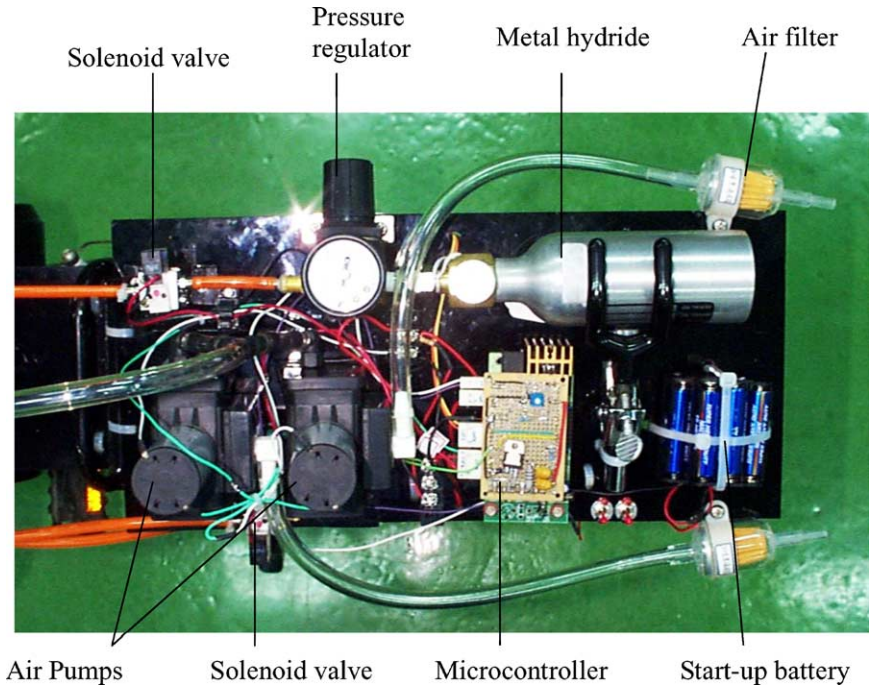

Fig. 3. Components on microcontroller.

by a fuel-cell stack with a large dynamic voltage (Fig. 1). The power supplied to the remaining components of the stack are regulated in terms of voltage by a dc–dc converter (Figs. 3 and 4).

2.2. Fuel-management sub-system

The fuel cells require hydrogen of at least 99.9% purity. As shown in Fig. 3 the storage system used for the fuel is hydrogen stored in the metal hydrides. Although, metal hydrides suffer from high alloy cost, sensitivity to gaseous impurities, and low gravimetric hydrogen density, they have excellent volumetric storage density together with an inherent advantage of being endothermic when releasing hydrogen, which thus reduces the risk of fire. In addition, the hydrogen is kept at a relatively low pressure (typically <10 atm) within the metal hydride canister rather than at high pressure (250 atm) as compressed gas in cylinders. Consequently, the rate of hydrogen leakage is less and the risks of explosion in the event of collision reduced [2,3].

In combination with a suitable pressure regulator, the metal hydrides provide a passive and simple load-following system. As shown in Fig. 1, hydrogen is provided to the system by a metal hydride canister and brought to the stack working pressure by a pressure regulator. A solenoid valve (V1) turns on as the pressure in the fuel feeding line decreases to a predetermined value (e.g., 7 psig) due to the electrochemical reaction. The exhaust line from the negative electrode (anode) is equipped with another solenoid valve (V2) which operates a conditional purge from the anode when the stack voltage is reduced to a predetermined value (e.g., 22 V) due to flooding.

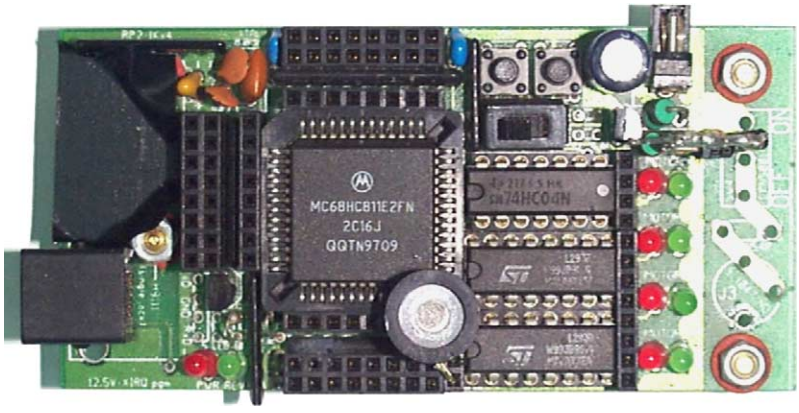

Fig. 4. 6811 single-chip microcontroller.

Table 3
Operation mode of air pumps

Mode	Cell current	Air pump 1	Air pump 2
Normal operation	$I < 7$ A	ON	OFF
	$I > 7$ A	ON	ON
Start/reset	–	ON	ON

Table 4
Operation of cooling sub-system

Mode	Stack temperature (°C)	Cooling fan action
Normal operation	$T < 35$	OFF
	$T > 40$	ON
Reset/shut-down	–	ON

2.3. Oxidant-management sub-system

Air is used as the oxidant at the positive electrode (cathode) of the fuel cell. Two air pumps are connected in parallel with the oxidant feeding line to deliver the oxidant to the fuel cell. Each air pump can blow about 12.5 l min^{-1} air into the feeding line. With a stoichiometric ratio of 2.5, this rate can support the cathode electrochemical reaction at a current of 7 A. As shown in Table 3, when the current passing through the stack is lower than 7 A, only one air pump is turned on to feed the cathodes in the stack with oxidant. When the current of the stack is higher than 7 A, the secondary air pump is also turned on to double the oxidant flow rate in the cathodes. Therefore, at any power level, the cathodic stoichiometric ratio is always higher than 2.5. Note that, the purpose of a high oxidant stoichiometric ratio in the cathode is not only to supply sufficient oxygen to the cathode but also to remove effectively, the by-product water. For start and reset, both air pumps are powered together for a short period (e.g., 2 s) to remove any water in the cathode.

2.3.1. Cooling sub-system

The fuel-cell stack is air-cooled by four turbofans that are trigged by the microcontroller according to the change in the surface temperature of stack. As shown in Table 4, when the temperature is higher than 40 °C, the cooling fans are turned on to remove the heat that is created by the electrochemical reaction. When the temperature of the stack surface is reduced to below 35 °C, the cooling fans are switched off for power saving. For reset and shut-down of the fuel-cell system, the cooling fans are kept at 'ON' for a short period (e.g., 20 s) (Table 4).

3. Microcontroller

A well-performed fuel-cell system relies not only on a high-quality stack, but also on an efficient control system together with proper automatic processes. The major task of this study is to develop a single-chip microcontroller to assure the proper operation of the fuel-cell electric bicycle. In the present system, a Motorola MC68HC811E2 microprocessor (Fig. 4) acts as the heart of the system. The instructions set to implement the control logic are stored in a 2 K EEPROM, to which any subsequent changes to the control strategy can be made easily. A watchdog timer circuit is employed to prevent any uncontrolled operation in the event of failure of the controller. All programming was performed in BASIC and in assembly language. The fixed, hardware-dependent drivers were written in assembly language for optimum speed and minimum memory use.

As shown in Fig. 1 and Table 5, the single-chip microcontroller is capable of monitoring the sensor signals of voltage (V), current (I), temperature (T), and pressure (P), and of appropriate actions to drive the external devices, i.e., the air pumps (S1, S2), solenoid valves (S3, S4), and cooling fan (S5). In addition, an LCD display is interfaced with the microcontroller to display the status of the fuel-cell system. The capability to monitor individual cell voltages is one of the most important functions of the microcontroller. A dedicated analog multiplexer with 40 channels monitors these voltages via electrical wires connected to the graphite current-collector plates. Monitoring of the total voltage alone does not provide sufficient information to detect the malfunction of an individual cell within the stack. A cell with a low voltage reading is an indication of a possibly hazardous condition, such as a gas leak in that cell, a perforated membrane, or a reversal in cell potential. For air operation, the individual cell voltages are normally between 0.6 and 1.0 V. A shut-down is performed if any cell voltage is below

Table 5
Summary of control system of fuel-cell electric bicycle

Category	Symbol	Name	Quantity	Function
Sensors	V	Voltage detect circuit	41	Detects cell and stack voltage
	I	Current detect circuit	1	Detects fuel-cell current
	T	Thermocouple	1	Measures fuel-cell temperature
	P	Pressure sensor	1	Measures hydrogen pressure in the feeding line
Actuators	S1, S2	Air pump	2	Provides oxidant to cathode
	S3, S4	Solenoid valves	2	Provides hydrogen and purges the exhaust
	S5	Cooling fan	4	Cools the fuel-cell stack
Microprocessor	–	MC68HC811E2	1	Control unit

Fig. 5. Roller-stand test of fuel-cell bicycle.

0.55 V. The differential voltage test is important because a defective or erratic cell can be detected before the fuel cell is subjected to a large load.

The basic functions performed by the microcontroller are as follows:

(i) Start-up of the power system of the fuel cell.
(ii) Monitoring of the power system to assure that it is within a predetermined overpotential envelope.
(iii) Shut-down of the power system in the event of system failure.

Typically, a fail-safe shut-down operation results from low cell voltage, low stack voltage, high stack temperature, or low hydrogen pressure. Start-up/shut-down includes the enabling/disabling of air pumps and solenoids.

4. Experimental

Two kinds of tests are undertaken in the present study, namely, the roller-stand test (Fig. 5) and the road test (Fig. 6).

Fig. 6. Road test of fuel-cell bicycle.

In the roller-stand test, the stack is fed with fuel from cylinders of compressed hydrogen while the hydrogen for the road test is delivered from two portable canisters of metal hydride. Usually, the motor of the electric bicycle can be operated under two different modes, i.e., the assistant mode and the independent mode. In the assistant mode, the electric motor assists the bicycle rider by providing a torque proportional to that given on the pedals, while the independent mode drives the electric motor in a similar fashion to that in a conventional electric scooter. In the present experiment, the independent mode is used in both the roller-stand and the road tests.

Data for the roller-stand test are given in Table 6. In the first few minutes, both the speed and the stack temperature gradually increase. After about 6 min, the fuel-cell system becomes steady, i.e., both the speed and the stack temperature remain constant. The maximum speed is about 25.2 km h^{-1} and the stack temperature varies between 30.0 and 31.9 °C. In general, the system displays reliable operation without any failure during the 1-h test. This indicates that the stability and reliability of the present control system are, to a certain extent, satisfactory.

Road-test data are listed in Table 7. In this test, the bicycle underwent a 2.5 km run inside ITRI, as shown in Fig. 6. The maximum speed of the road test was about 16.8 km h^{-1}, i.e., lower than that of the roller-stand test. This is because there is a rider on the electric bicycle in the road test and therefore the weight is higher than in the roller-stand test. In addition, the drag caused by the air stream in the road test could reduce the maximum speed. On the other

Table 6
Performance of the fuel-cell bicycle under roller-stand test

Distance (km)	Time (min)	Speed (km h^{-1})	Stack temperature (°C)	Remarks
0	0	0	23.2	Check
0.29	1.02	18.3	26.0	
0.65	2.01	23.9	27.7	
1.04	3.01	24.5	28.5	Stack temperature gradually increases
1.43	4.01	25.2	29.3	
1.82	5.00	25.2	29.4	
2.21	6.00	25.2	30.1	
2.60	7.00	25.2	30.0	Stack temperature becomes steady
3.00	7.59	25.2	30.5	
3.40	9.00	25.2	30.3	
3.80	9.59	25.2	30.9	
4.19	11.01	25.2	31.1	Stack temperature is varied between 30 and 32 °C
5.39	21.01	25.2	31.9	
8.28	30.00	26.0	30.8	
12.61	40.01	25.1	31.4	
16.78	49.99	26.2	30.7	
21.03	60.00	25.2	31.6	Stop

Test conditions: bicycle weight, 30 kg; room temperature, 22.3 °C; H_2 pressure, 7 psig; oxidant stoichiometric ratio > 2.5.

Table 7
Records of the road test for the fuel-cell electric bicycle

Distance (km)	Time (min)	Speed (km h^{-1})	Stack temperature (°C)	Remarks
0	0	0	23.1	Check pipe and electric lines; then start
0.28	1.54	13.3	24.5	Stack temperature gradually increases
1.10	6.20	15.9	30.1	Water condenses on canister surface
1.47	8.20	15.9	30.2	Water becomes cool and frost
2.20	12.29	16.2	29.2	Stack temperature becomes steady
3.15	17.23	16.2	30.3	Steady
4.51	22.32	16.2	30.2	Steady
6.68	27.30	16.8	29.8	Steady
7.82	32.91	16.4	30.0	H_2 pressure gradually decreases
9.18	38.14	16.2	30.3	H_2 pressure approaches 0 psig and motor slows down

Test conditions: bicycle weight, 30 kg; rider weight, 70 kg; hydrogen consumption, 6.8 g; ambient temperature, 22.6 °C; H_2 pressure, 7 psig; oxidant stoichiometric ratio > 2.5.

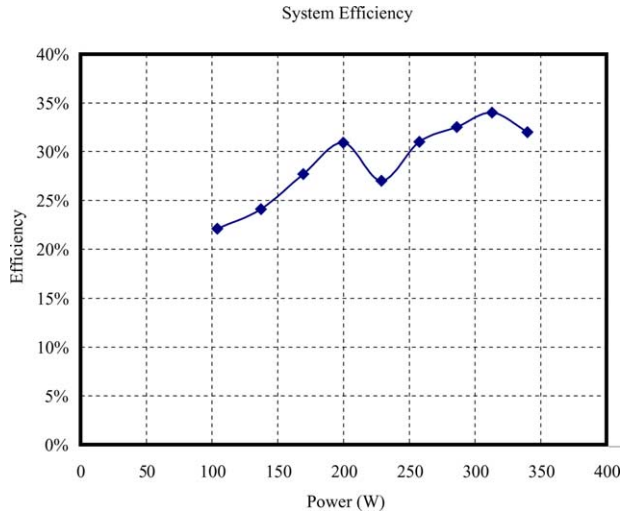

Fig. 7. System efficiency of fuel-cell bicycle.

hand, the forced convection by the air stream reduces the stack temperature by 1–2 °C. The amount of hydrogen delivered from the metal hydrides is calculated by the weight loss of the canister. The content of hydrogen is about 3.4 g per canister. Therefore, a total of 6.8 g hydrogen covers the driving distance of 9.18 km, meaning that the present electric bicycle has a distance-to-fuel ratio of 1.35 km g^{-1} H_2.

The efficiency of the fuel-cell system as a function of the gross power output is shown in Fig. 7. The system efficiency is defined as the ratio of net power delivered by the fuel cell to the enthalpy flow of the consumed hydrogen. The general trend of the system efficiency is a slight increase with increasing gross power output. At a gross power of 200 W, however, the system efficiency is decreased. This is because of the activation of the secondary air pump. Under nominal conditions, the system efficiency is about 35%, which is significantly higher than that of an internal-combustion engine.

5. Conclusions

Phase I of the Mingdao Fuel Cell Project has been completed with the development of a fuel-cell-powered electric bicycle. The information and experience obtained with the design, fabrication, and testing of this prototype will assist further advancement of the fuel-cell technology. The bicycle may also prove useful for enhancing public acceptance of hydrogen fuel, and for facilitating the licensing processes of this technology. Phase II, i.e., development of two-seater, lightweight, fuel-cell vehicle, is ready to commence. The final goal of this project is to promote proton exchange membrane fuel cell (PEMFC) technology and accelerate it to commercialization, thus making it accessible to all applications that require a clean and efficient source of energy.

Acknowledgements

This work was partly sponsored by National Science Council of Taiwan under contract no. NSC 92-2212-E451-002.

References

[1] J.J. Hwang, H.S. Hwang, J. Power Sources 104 (2002) 24–32.
[2] D. Browning, P. Jones, K. Packer, J. Power Sources 65 (1997) 187–195.
[3] B.D. James, G.N. Baum, F.D. Lomax, C.E. Thomas, I.F. Kuhn Jr., Comparison of onboard hydrogen storage for fuel cell vehicles, Task 4.2 Final Report, Directed Technologies, prepared for Ford Motor Company under Prime Contract DE-AC02-94CE50389 to the US DOE.